Inorganic Chemistry

ARTICLE

pubs.acs.org/IC

Facile Reduction of a Uranyl(VI) β-Ketoiminate Complex to U(IV) Upon Oxo Silylation

Jessie L. Brown, Charles C. Mokhtarzadeh, Jeremie M. Lever, Guang Wu, and Trevor W. Hayton*

Department of Chemistry and Biochemistry, University of California Santa Barbara, Santa Barbara, California 93106, United States

Supporting Information

ABSTRACT: Reaction of the uranyl β-ketoiminate complex $UO_2(^{tBu}acnac)_2$ (**1**) ($^{tBu}acnac$ = $^{t}BuNC(Ph)CHC(Ph)O$) with Me_3SiI, in the presence of Ph_3P, results in the reductive silylation of the uranyl moiety and formation of the U(V) *bis*-silyloxide complex $[Ph_3PI][U(OSiMe_3)_2I_4]$ (**2**). Subsequent reaction of **2** with Lewis bases, such as 2,2′-bipyridine (bipy), 1,10-phenanthroline (phen), and tetrahydrofuran (THF), results in a further reduction of the metal center and isolation of the U(IV) complexes $U(OSiMe_3)_2I_2(bipy)_2$ (**3**), $U(OSiMe_3)_2I_2(phen)_2$ (**4**), and $[U(OSiMe_3)_2I(THF)_4][I_3]$ (**5**), respectively.

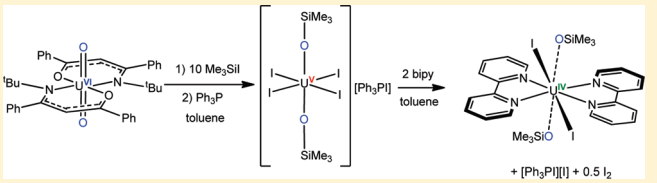

INTRODUCTION

Reductive silylation of the uranyl moiety (UO_2^{2+}) is one of the few synthetic procedures available for functionalizing this normally unreactive fragment.[1−3] This reaction involves silylation of either one or both uranyl oxo ligands with concomitant reduction of the uranium center to U(V) or U(IV). For example, Arnold and co-workers observed reductive silylation of $UO_2(THF)(K_2L)$ (L = "Pacman" polypyrrolic macrocycle) by $HN(SiMe_3)_2$, forming the U(V) silyloxide $[UO(OSiMe_3)(THF)Fe_2I_2L]$ as the final product.[1,4−6] During the reaction, $HN(SiMe_3)_2$ acts as both the reductant and the silylating reagent. We recently reported a similar transformation, namely, that addition of excess Me_3SiI to $UO_2(^{Ar}acnac)_2$ ($^{Ar}acnac$ = $ArNC(Ph)CHC(Ph)O$, Ar = 3,5-$^{t}Bu_2C_6H_3$) results in the formation of the U(V) *bis*-silyloxide $U(OSiMe_3)_2I_2(^{Ar}acnac)$.[2] This material is formed by reduction of the uranium center concomitant with silylation of *both* oxo ligands. We postulated that coordination of Me_3Si^+ to the uranyl oxo ligand substantially increases the uranium oxidation potential, allowing it to oxidize the iodide anion. Consistent with this hypothesis we observed the formation of I_2 in the reaction mixture. Ephritikhine and co-workers have also observed the reductive silylation of uranyl. Specifically, the addition of excess of Me_3SiX (X = Br, Cl, I) to either $UO_2(OTf)_2$ or $UO_2I_2(THF)_3$, in acetonitrile, results in complete removal of the oxo ligands, and the formation of the U(IV) complexes, $UX_4(MeCN)_4$.[3] In each of these examples, reductive silylation is driven by the formation of strong Si−O bonds in combination with the presence of weaker Si−X bonds (either Si−I or Si−N).[7] However, the presence of an easily oxidizable substrate (to generate the U(V) center) also plays a role in the transformations.

Herein we report another example of reductive silylation in uranyl and explore the reactivity of the functionalized product. In particular, the reaction of the uranyl β-ketoiminate complex $UO_2(^{tBu}acnac)_2$ (**1**) ($^{tBu}acnac$ = $^{t}BuNC(Ph)CHC(Ph)O$) with Me_3SiI, in the presence of Ph_3P, results in the reductive silylation of the uranyl moiety and formation of $[Ph_3PI][U(OSiMe_3)_2I_4]$ (**2**). Interestingly, complex **2** reacts with Lewis bases to undergo further reduction, ultimately generating a U(IV) *bis*-silyloxide complex and iodine.

RESULTS AND DISCUSSION

We have been exploring the ability of the diphenyl-β-ketoiminate ligand platform to coordinate the UO_2^{2+} moiety,[8,9] as this ligand class creates a bulky, substitutionally inert ligand environment that prevents further coordination of Lewis bases to the uranyl equatorial plane. Moreover, the strongly electron-donating properties of this ligand set appear to activate the uranyl oxo ligands toward functionalization.[8] To increase the electron-donating capability of the ligand, and consequently the nucleophilicity of the oxo ligands, we have endeavored to install an electron-donating *tert*-butyl substituent on the nitrogen atom of the diphenyl-β-ketoimine. The synthesis of β-ketoimines is normally achieved by condensation of a β-diketone with a primary amine.[10−14] However, the reaction of *tert*-butylamine with dibenzoylmethane does not result in formation of a β-ketoimine, presumably because of an unfavorable steric interaction between the *tert*-butyl substituent and the phenyl ring of the dibenzoylmethane. As a result, an alternate synthetic route for the preparation of a *tert*-butyl substituted diphenyl-β-ketoimine was utilized, namely, reaction of excess *tert*-butylamine with diphenylpropynone, in the presence of 10 mol % $Zn(OTf)_2$.[14] After heating the reaction mixture to reflux for 48 h, $^{t}BuNHC(Ph)CHC(Ph)O$, ($^{tBu}acnac$)H, could be isolated as a yellow solid in 86% yield (Scheme 1). The ^1H NMR spectrum of ($^{tBu}acnac$)H in C_6D_6 (see the Supporting Information, Figure S12) exhibits a singlet at 1.00 ppm, assignable to the methyl

Received: February 23, 2011
Published: May 05, 2011

Scheme 1

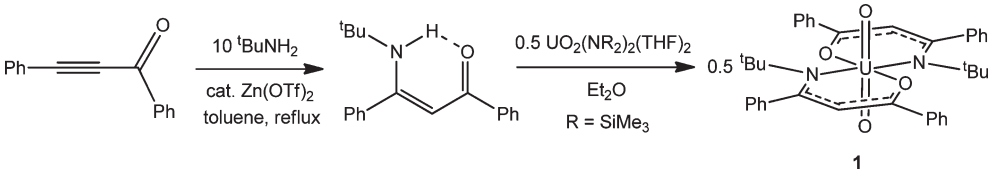

Scheme 2

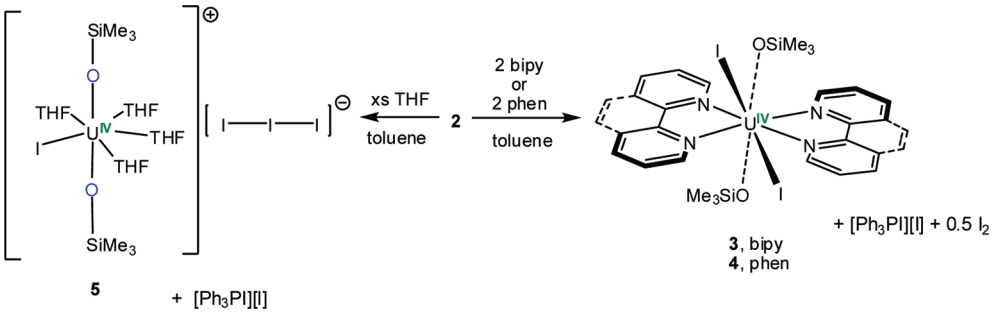

groups of the ^{t}Bu moiety, while the amine proton is observed at 12.32 ppm.

Reaction of (^{tBu}acnac)H in Et_2O with 0.5 equiv of UO_2(N-{$SiMe_3$}$_2$)$_2$(THF)$_2$ results in the deposition of UO_2(^{tBu}acnac)$_2$ (**1**) an orange microcrystalline solid in 67% yield (Scheme 1). Complex **1** is partly soluble in Et_2O and toluene, but reasonably soluble in tetrahydrofuran (THF) and CH_2Cl_2. Its ^{1}H NMR spectrum in C_6D_6 exhibits a singlet at 1.73 ppm, assignable to the methyl groups of the ^{t}Bu moiety, while the proton attached to the γ-carbon of the ketoiminate ring is observed at 5.81 ppm (Supporting Information, Figure S14). The IR spectrum of **1** (in Nujol) exhibits a vibration at 907 cm^{-1}, assignable to ν_{asym}(U═O), while the Raman spectrum exhibits a strong vibration at 823 cm^{-1}, assignable to ν_{sym}(U═O) (Supporting Information, Figures S1 and S6, respectively). Surprisingly, the latter assignment is higher that that observed for UO_2(^{Ar}acnac)$_2$ (Ar = 3,5-^{t}Bu$_2$C$_6$H$_3$) [ν_{sym}(U═O) = 812 cm^{-1}] (Supporting Information, Figure S7), despite the stronger donating capacity of the *tert*-butyl substituent in **1**.

Crystals of **1** suitable for X-ray analysis were grown from a dichloromethane/hexane solution. Complex **1** crystallizes in the triclinic space group $P\bar{1}$ as a dichloromethane solvate, **1**·2CH_2Cl_2. Its solid-state molecular structure is shown in Figure 1, while the crystallographic details are found in Table 1. Complex **1** exhibits a slightly distorted octahedral geometry about the uranium center in which two β-ketoiminate ligands occupy the equatorial plane. As observed in other uranyl β-ketoiminate complexes, the *N*-*tert*-butyl substituents in **1** exhibit a trans configuration.[8] Its U−O(oxo) bond length (U1−O1 = 1.770(3) Å) and O−U−O bond angle (O1−U1−O1* = 180°) are typical of uranyl(VI) complexes. Interestingly, the U−N bond length in **1** (U1−N1 = 2.531(3) Å) is longer than the comparable bond length in UO_2(^{Ar}acnac)$_2$ (U1−N1 = 2.449(6) Å),[8] likely because of the greater steric demand of the *tert*-butyl substituent.

Solution-phase cyclic voltammetry was carried out on **1** to ascertain its redox properties (Supporting Information, Table S1).

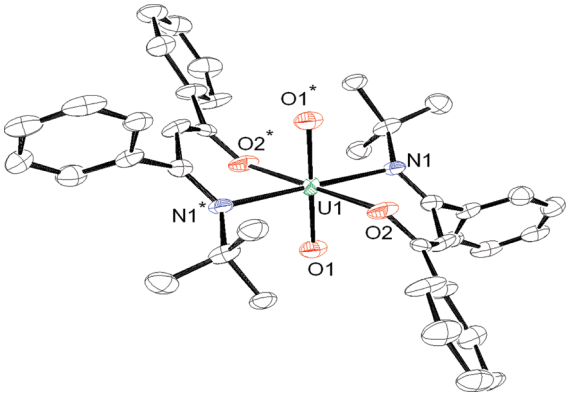

Figure 1. Molecular structure of UO_2(^{tBu}acnac)$_2$ (**1**·2CH_2Cl_2) with 50% probability ellipsoids. CH_2Cl_2 and hydrogen atoms omitted for clarity. Selected bond lengths (Å) and angles (deg): U1−O1 = 1.770(3), U1−O2 = 2.228(2), U1−N1 = 2.531(3), O1−U1−O1* = 180, O2−U1−N1 = 75.28(9), O2−U1−N1* = 104.72(9).

The cyclic voltammogram of **1** in CH_2Cl_2 reveals a reversible reduction feature at $E_{1/2}$ = −1.46 V (vs Fc/Fc$^+$), which we attribute to the U(VI)/U(V) redox couple (Figure 2). This reduction potential lies between those reported previously for the other uranyl β-ketoiminate complexes. For example, UO_2-(^{Ar}acnac)$_2$ (Ar = 3,5-^{t}Bu$_2$C$_6$H$_3$) exhibits a U(VI)/U(V) reduction potential at −1.35 V, while UO_2(^{Ar}acnac)$_2$ (Ar = 2,4,6-Me$_3$C$_6$H$_2$) exhibits a U(VI)/U(V) reduction potential at −1.52 V.[8] In addition, the observed potential for **1** is smaller than that seen for [UO_2(salan-^{t}Bu$_2$)(py)] (−1.81 V),[15] but similar to most other uranyl Schiff-base complexes.[15,16] Overall, the cyclic voltammetry data, in combination with the Raman spectroscopic results, suggests that coordination of the *tert*-butyl-substituted β-ketoiminate ligand does not result in a more electron-rich uranium center than that observed with the aryl-substituted β-ketoiminates, likely because the longer

dx.doi.org/10.1021/ic200387n |*Inorg. Chem.* 2011, 50, 5105–5112

Table 1. X-ray Crystallographic Data for Complexes 1·2CH_2Cl_2, 2, 3·CH_2Cl_2, and 5

	1·2CH_2Cl_2	2	3·CH_2Cl_2	5
empirical formula	$UO_4C_{40}H_{44}N_2Cl_4$	$UO_2C_{24}H_{33}Si_2P_1I_5$	$UO_2C_{27}H_{36}N_4Si_2I_2Cl_2$	$UO_6C_{22}H_{50}Si_2I_4$
crystal habit, color	block, orange	block, black	block, orange	block, orange
crystal size (mm)	0.20 × 0.20 × 0.05	0.2 × 0.2 × 0.30	0.8 × 0.3 × 0.2	0.20 × 0.10 × 0.05
crystal system	triclinic	triclinic	monoclinic	triclinic
space group	$P\bar{1}$	$P\bar{1}$	$C2/c$	$P\bar{1}$
volume ($Å^3$)	996.1(4)	1879(3)	3533(2)	1907.3(12)
a (Å)	9.5091(19)	9.452(7)	20.377(7)	9.519(4)
b (Å)	9.552(2)	9.961(8)	9.122(3)	12.725(5)
c (Å)	11.408(2)	20.940(16)	19.007(6)	16.355(6)
α (deg)	98.382(3)	103.327(12)	90.00	89.944(6)
β (deg)	97.715(3)	90.511(13)	90.883(6)	74.313(6)
γ (deg)	99.983(3)	101.222(12)	90.00	89.970(6)
Z	1	2	4	2
formula weight (g/mol)	996.60	1313.18	1065.49	1212.43
density (calculated) (Mg/m^3)	1.661	2.321	2.003	2.111
absorption coefficient (mm^{-1})	4.384	8.553	6.591	7.583
F_{000}	490	1186	2000	1124
total no. reflections	8559	15723	15034	16397
unique reflections	3968	7383	3848	7615
R_{int}	0.0487	0.1135	0.0740	0.0803
final R indices [$I > 2\sigma(I)$]	R_1 = 0.0333	R_1 = 0.0494	R_1 = 0.0389	R_1 = 0.0483
	wR_2 =0.0651	wR_2 = 0.1216	wR_2 = 0.0892	wR_2 = 0.1224
largest diff. peak and hole ($e^- Å^{-3}$)	1.261 and −0.772	3.346 and −4.095	3.311 and −1.381	1.869 and −2.275
GOF	1.015	1.004	1.088	0.973

U−N bonds found in **1** result in relatively poor U−N orbital overlap.

To ascertain the nucleophilicity of the uranyl oxo ligands in **1** we have explored its reactivity with electrophiles. Addition of excess Me_3SiI to **1** in toluene produces a deep red solution. Subsequent addition of Ph_3P to the reaction mixture results in the deposition of a black solid. Recrystallization of this solid from CH_2Cl_2 at −25 °C affords the U(V) *bis*-silyloxide complex, $[Ph_3PI][U(OSiMe_3)_2I_4]$ (**2**), in 40% yield (eq 1).

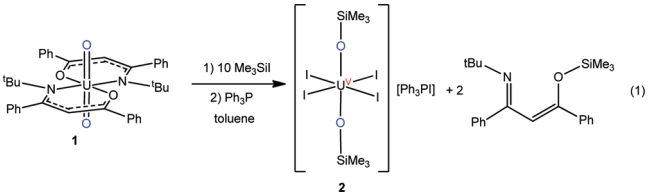

Complex **2** crystallizes in the triclinic space group $P\bar{1}$ as a discrete anion/cation pair, and its solid-state molecular structure is shown in Figure 3. Further crystallographic details for **2** can be found in Table 1. The uranium center in the $[U(OSiMe_3)_2I_4]^-$ anion exhibits an octahedral geometry, in which four iodide ligands occupy the equatorial plane, while the oxo-derived silyloxide ligands occupy the axial positions (O1−U1−O1* = 180°). The U−O($SiMe_3$) bond length (U1−O1 = 1.990(6) Å) is similar to those in previously reported U(V) silyloxide complexes,[1,2] and is much longer than the U═O bond lengths typically observed for uranyl. In addition, the Si1−O1 (1.688(8) Å) and U−I (U1−I1 = 2.9841(19) Å, U1−I2 = 2.999(2) Å) bond lengths in **2** are comparable with those reported for $U(OSiMe_3)_2I_2$-(^{Ar}acnac) (Ar = 3,5-^{t}Bu$_2$C$_6$H$_3$).[2] Finally, the metrical parameters of the phosphonium cation, $[Ph_3PI]^+$, are similar to those observed previously.[17−21]

The ^{1}H NMR spectrum of complex **2** in CD_2Cl_2 exhibits a broad resonance at 4.03 ppm, assignable to the Me_3Si protons of the oxo-derived silyloxide ligands, while the ^{1}H resonances of the $[Ph_3PI]^+$ moiety are observed at 7.38 ppm, 7.61 ppm, and 7.77 ppm, assignable to the *ortho*, *meta*, and *para* positions, respectively. Interestingly, a second singlet, at 2.17 ppm, is observed in the ^{1}H NMR spectrum, which is also assignable to an $SiMe_3$ resonance. This peak is present in all samples of **2**, and is always observed in a 1:3 ratio with respect to the resonance at 4.03 ppm. This ratio does not change appreciably upon cooling to −60 °C. Given this, we suggest that the two resonances are indicative of the presence of cis and trans isomers in solution. Alternately, this behavior could be due to iodide dissociation from complex **2**; however, addition of 2 equiv of $[Ph_3PI][I]$ to an NMR sample of **2** does not affect the two $SiMe_3$ resonances, arguing that I-dissociation is not occurring. Complex **2** slowly decomposes in solution, and upon standing in CD_2Cl_2 for 24 h, its ^{1}H NMR spectrum reveals the appearance of a new resonance at 0.09 ppm, attributable to the formation of $Me_3SiOSiMe_3$, while the resonances assignable to **2** are decreased in intensity.

The magnetic moment of **2** (μ_{eff} = 1.4 μ_B at 295 K), determined via Evans' method,[22] is much lower than the theoretical value of 2.54 μ_B,[23] but is comparable to the magnetic moments of other U(V) complexes,[24] including $U(OSiMe_3)_2I_2(^{Ar}acnac)$ (μ_{eff} = 1.52 μ_B at 298 K).[2] Finally, the NIR spectrum for complex **2** is consistent with the presence of a $5f^1$ ion (Supporting Information, Figure S9).[15,25,26]

We also explored the mechanism of formation of complex **1**. An in situ ^{1}H NMR spectrum of the reaction mixture in C_6D_6,

dx.doi.org/10.1021/ic200387n |*Inorg. Chem.* 2011, 50, 5105–5112

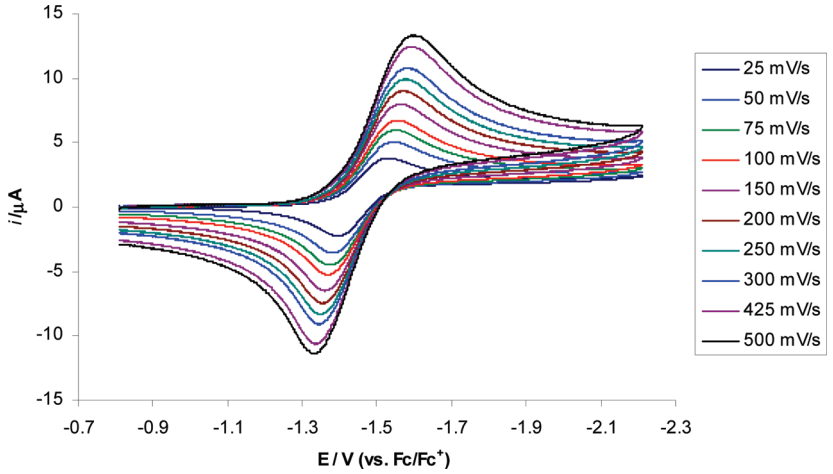

Figure 2. Room temperature cyclic voltammogram for **1** in CH_2Cl_2 (vs Fc/Fc^+, 0.1 M $[NBu_4][PF_6]$ as supporting electrolyte).

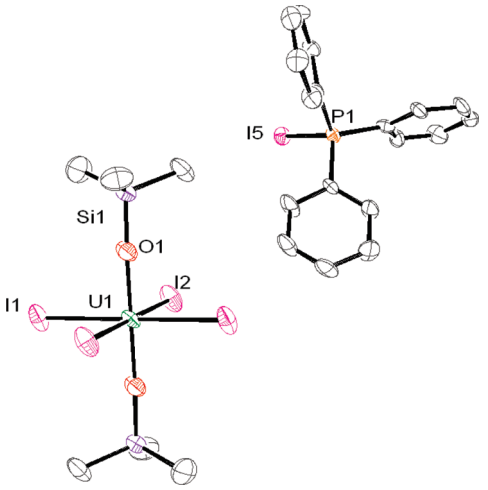

Figure 3. Molecular structure of $[Ph_3PI][U(OSiMe_3)_2I_4]$ (**2**) with 50% probability ellipsoids. Hydrogen atoms omitted for clarity. Selected bond lengths (Å) and angles (deg): U1−O1 = 1.990(6), U1−I1 = 2.9841(19), U1−I2 = 2.999(2), O1−Si1 = 1.688(8), P1−I5 = 2.408(3), O1−U1−O1* = 180, O1−U1−I1 = 90.4(2).

before addition of Ph_3P, revealed the presence of a broad singlet at 5.03 ppm (Supporting Information, Figure S15), suggesting the formation of a uranium silyloxide complex. However, all attempts to isolate this intermediate species have proven unsuccessful because of its high solubility. Also observed in this spectrum are two resonances at −0.24 ppm and +1.48 ppm, in a 1:1 ratio, assignable to the Me_3Si and ^tBu protons, respectively, of $^tBuNC(Ph)CHC(Ph)OSiMe_3$. This is in agreement with the independently prepared material, formed via reaction of Na(^{tBu}acnac) with 2 equiv of Me_3SiCl.[13] Thus, 4 equiv of Me_3SiI are formally required for the formation of **2**, as 2 equiv are required for silylation of each oxo ligand and 2 equiv are required for silylation of each β-ketoiminate ligand. The extra steric bulk of the *tert*-butyl substituted β-ketoiminate likely makes ligand abstraction more facile than its aryl-substituted counterpart,[2] accounting for the loss of both ^{tBu}acnac ligands from the product.

As observed in previous silylation reactions, the uranium center in **1** is reduced to U(V). We suspect that the oxo ligand silylation alters the redox potential of the U^{6+} center, making the U^{6+} ion more oxidizing. As a consequence, one iodide anion is oxidized by uranium, forming 0.5 equiv of iodine and an intermediate U(V) species, presumably $U(OSiMe_3)_2I_3$. The iodine then reacts with Ph_3P to form the iodophosphonium salt, $[Ph_3PI][I]$,[17] which is subsequently trapped by $U(OSiMe_3)_2I_3$ to give the final product, complex **2**. Because only 0.5 equiv of I_2 is generated in the reduction to U(V), and a full equiv of I_2 is required to form $[Ph_3PI][I]$, the maximum yield of **2** can only be 50%.

We have endeavored to explore the reactivity of complex **2** with Lewis bases to better understand the coordination chemistry of the uranyl-derived U(V) silyloxides. Addition of 2 equiv of 2,2′-bipyridine (bipy) to a suspension of **2** in toluene results in a color change to orange, concomitant with the deposition of a dull yellow solid. The yellow solid was determined to be $[Ph_3PI][I]$ by both ^1H and ^{31}P NMR spectroscopy, while a U(IV) complex, $U(OSiMe_3)_2I_2(bipy)_2$ (**3**), could be isolated from the supernatant in good yield as an orange microcrystalline powder (Scheme 2). Similarly, addition of 1,10-phenanthroline (phen) to a toluene suspension of **2** generates $U(OSiMe_3)_2I_2(phen)_2$ (**4**), in moderate yields. The reductant in these transformations is likely iodide, which would result in the formation of 0.5 equiv of I_2 over the course of the reactions.

Single crystals of **3** suitable for X-ray diffraction analysis were grown from a 1:4 mixture of CH_2Cl_2 and hexane. Complex **3** crystallizes in the monoclinic space group *C*2/*c* as a dichloromethane solvate, $3\cdot CH_2Cl_2$, and its solid-state molecular structure is shown in Figure 4. Complex **3** exhibits a dodecahedral geometry, in which the two orthogonal trapezoids are defined by O1−N2−N1−I1 and O1*−N2*−N1*−I1*.[27] The U−O(silyloxide) bond length (U1−O1 = 2.084(4) Å) in **3** is longer than that observed in **2**, in accord with the larger radius of the U^{4+} ion and the higher coordination number. Interestingly, the O1−U1−O1* bond angle in **3** (115.5(2)°) is substantially smaller than the O−U−O angle observed in either **2** (O1−U1−O1* = 180°) or a typical uranyl complex. The U−I bond length (U1−I1 = 3.2435(8) Å) in **3** is significantly elongated relative to **2** (U1−I1 = 2.9841(19) Å), while the U−N bond lengths in **3** (2.646(5) Å and 2.670(5) Å) are typical of other reported U−N(bipy) bond distances.[28−31]

The ^1H NMR spectrum of complex **3** in CD_2Cl_2 exhibits a broad resonance at 52.14 ppm, assignable to the Me_3Si protons of the silyloxide ligands, while the proton at the 3-position of the bipyridine ring is observed as a broad singlet

dx.doi.org/10.1021/ic200387n |*Inorg. Chem.* 2011, 50, 5105–5112

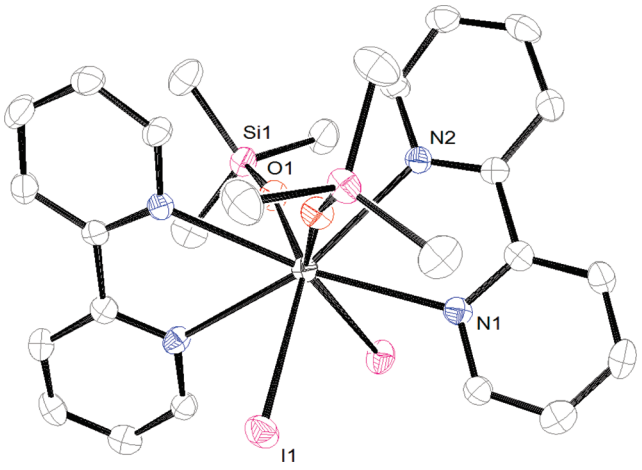

Figure 4. Molecular structure of $U(OSiMe_3)_2I_2(bipy)_2$ (**3**·CH_2Cl_2) with 50% probability ellipsoids. CH_2Cl_2 and hydrogen atoms omitted for clarity. Selected bond lengths (Å) and angles (deg): U1−O1 = 2.084(4), U1−I1 = 3.2435(8), O1−Si1 = 1.639(4), O1−U1−O1* = 115.5(2), I1−U1−I1* = 98.72(3), U1−O1−Si1 = 165.4(3).

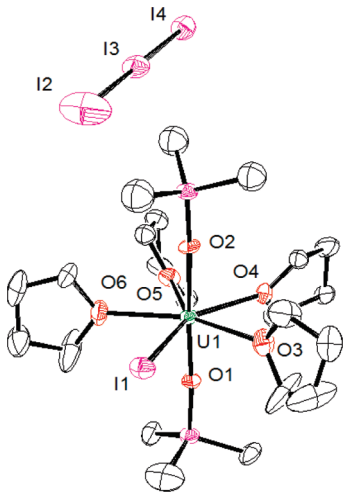

Figure 5. Molecular structure of $[U(OSiMe_3)_2I(THF)_4][I_3]$ (**5**) with 50% probability ellipsoids. Hydrogen atoms omitted for clarity. Selected bond lengths (Å) and angles (deg): U1−O1 = 2.065(6), U1−O2 = 2.080(6), O1−Si1 = 1.670(6), O2−Si2 = 1.659(6), U1−I1 = 3.1445(13), U1−O6 = 2.472(7), O1−U1−O2 = 173.8(3), U1−O1−Si1 = 170.0(4), O1−U1−O6 = 90.4(2), O1−U1−I1 = 93.95(18).

at −28.68 ppm (Supporting Information, Figure S17). The remaining protons of the bipyridine moiety are observed at −19.63 ppm, −3.01 ppm, and −2.75 ppm. Not surprisingly, the ^{1}H NMR spectrum of **4** in CD_2Cl_2 (Supporting Information, Figure S18) is similar to that of **3**, while the NIR spectra of complexes **3** and **4** are consistent with other U(IV) complexes.[32−34] Finally, the effective magnetic moment of **3** (2.7 μ_B at 295 K),[22] is greater than that observed for **2**, and suggestive of a $5f^2$ electronic configuration.[23,35,36]

The reactivity of complex **2** with monodentate Lewis bases was also explored. For instance, addition of 30 equiv of THF to a CD_2Cl_2 solution of **2** results in the immediate formation of a bright orange solution. This new material exhibits a singlet in its ^{1}H NMR spectrum at 63.2 ppm, assignable to the methyl groups of the silyloxide ligand. The chemical shift of this resonance suggests reduction of the uranium center to U(IV), as was observed for complexes **3** and **4**. Also present in these samples are small amounts of $Me_3SiOSiMe_3$, as revealed by the presence of a resonance at 0.12 ppm. This peak was confirmed to be $Me_3SiOSiMe_3$ by comparison with an authentic sample. On standing at room temperature, the signal at 63.2 ppm decreases in intensity, while the $Me_3SiOSiMe_3$ signal increases. New signals at 58.5 ppm and 53.4 ppm also begin to appear in the ^{1}H NMR spectrum. Similar results are observed upon dissolution of **2** into THF-d_8. However, under these conditions the disappearance of the signal at 63.2 ppm and the appearance of $Me_3SiOSiMe_3$ occur at a much faster rate.

Crystallization of the solution formed upon dissolution of **2** in THF, by layering with hexane, generates a mixture of orange needles and yellow needles. The yellow needles were identified as $[Ph_3PI][I]$ by comparison of the ^{31}P and ^{1}H NMR spectra with an authentic sample, while the orange needles were identified as $[U(OSiMe_3)_2I(THF)_4][I_3]$ (**5**) by X-ray crystallography (Scheme 2). Complex **5** crystallizes in the triclinic space group $P\bar{1}$ as a discrete anion/cation pair, and its solid-state molecular structure is shown in Figure 5. The uranium center in complex **5** exhibits a pentagonal bipyramidal geometry in the solid-state. The two silyloxide ligands occupy the axial coordination sites (O1−U1−O2 = 173.8(3)°), while four THF molecules and one iodide ligand occupy the equatorial plane. The U−O(silyloxide) bond distances (U1−O1 = 2.065(6) Å and U1−O2 = 2.080(6) Å) are nearly identical to those observed in **3**. In addition, the metrical parameters of the triiodide anion, I_3^-, are similar to previously reported values.[37] Most importantly, the presence of the I_3^- anion in **5** indicates that I_2 is being formed upon addition of THF, and confirms that iodide can reduce U(V) to U(IV) upon addition of Lewis bases to complex **2**.

A ^{1}H NMR spectrum (in CD_2Cl_2) of the material isolated by crystallization reveals a broad singlet at 58.10 ppm, which is similar to one of the resonances observed in the in situ experiment. We have assigned this resonance to the silyloxide groups of complex **5**. As was observed in the in situ experiment, the material is thermally unstable, and upon standing the resonance at 58.10 ppm decreases in intensity, while the resonance assignable to $Me_3SiOSiMe_3$ increases. Clearly the decomposition of **5** is driven by formation of hexamethyldisiloxane, presumably formed by scrambling of the Me_3Si^+ groups. It is also possible that its relatively high sensitivity may be due to the ability of uranium(IV) iodide complexes to ring-open THF.[38] Unfortunately, further attempts to characterize complex **5** were complicated by its thermal instability and its similar solubility with $[Ph_3PI][I]$. Consequently, we could not determine a yield. However, owing to the fact that only 0.5 equiv of I_2 is generated in the reaction, the maximum yield of **5** is 50%.

SUMMARY

Reaction of $UO_2(^{tBu}acnac)_2$ with excess Me_3SiI, in the presence of Ph_3P, results in reductive silylation of the uranyl moiety to afford the U(V) *bis*-silyloxide complex, $[Ph_3PI][U(OSiMe_3)_2I_4]$. Addition of Lewis bases to $[Ph_3PI][U(OSiMe_3)_2I_4]$ induces a second one-electron reduction and formation of a U(IV) *bis*-silyloxide complex. Normally the 6+ uranyl ion is a challenge to reduce to U(V) or U(IV);[39] however, our results reveals that a rich redox chemistry can be accessed by silylation of the uranyl moiety. This is because the oxo-derived silyloxide ligands are not as adept as oxo ligands at stabilizing a 6+ or 5+ charge on

dx.doi.org/10.1021/ic200387n |*Inorg. Chem.* 2011, 50, 5105–5112

uranium, an observation which is further highlighted by the fact that the reductant in the process, I^-, is a relatively mild reducing agent. In addition, the formation of $U(OSiMe_3)_2I_2(bipy)_2$ from uranyl parallels the synthesis of $UX_4(MeCN)_4$ (X = Cl, Br, I), reported by Ephritikhine and co-workers,[3] and it is likely that $[U(OSiMe_3)_2I_4]^-$ and $U(OSiMe_3)_2I_2(bipy)_2$ are analogous to the intermediates generated along the pathway to $UX_4(MeCN)_4$. Ultimately, the observed redox chemistry reveals the importance of functionalizing the uranyl oxo ligands to access the 4+ state, an observation which may have implications for the bioremediation of uranyl in the environment or the separation of uranyl in spent nuclear waste.

EXPERIMENTAL SECTION

General Procedures. All reactions and subsequent manipulations were performed under anaerobic and anhydrous conditions under either high vacuum or an atmosphere of nitrogen or argon. THF, hexanes, Et_2O, and toluene were dried using a Vacuum Atmospheres DRI-SOLV solvent purification system. CH_2Cl_2 and CD_2Cl_2 were dried over 3 Å molecular sieves for 24 h before use. C_6D_6 was dried over activated 4 Å molecular sieves for 24 h before use. $UO_2(N\{SiMe_3\}_2)_2(THF)_2$ was synthesized according to the previously reported procedure.[40] $UO_2(^{Ar}acnac)_2$ (Ar = 3,5-$^tBu_2C_6H_3$) was also synthesized according to the previously reported procedure.[8] This complex exhibits a $\nu_{sym}(U{=}O)$ at 812 cm^{-1} (see Supporting Information, Figure S7). All other reagents were purchased from commercial suppliers and used as received.

NMR spectra were recorded on a Varian UNITY INOVA 400 or Varian UNITY INOVA 500 spectrometer. ^1H and $^{13}C\{^1H\}$ NMR spectra were referenced to external $SiMe_4$ using the residual protio solvent peaks as internal standards (^1H NMR experiments) or the characteristic resonances of the solvent nuclei (^{13}C NMR experiments). $^{31}P\{^1H\}$ NMR spectra were referenced to external 85% H_3PO_4. IR spectra were recorded on a Mattson Genesis FTIR spectrometer. Raman spectra were recorded on a Nicolet 6700 FTIR spectrometer with a NXR FT Raman Module. UV−vis/NIR experiments were performed on a UV-3600 Shimadzu spectrophotometer. Magnetic moments were determined using the Evans' method.[22] Elemental analyses were performed by the Micro-Mass Facility at the University of California, Berkeley.

Cyclic Voltammetry Measurements. CV experiments were performed with a CH Instruments 600c Potentiostat, and the data were processed using CHI software (version 6.29). All experiments were performed in a glovebox using a 20 mL glass vial as the cell. The working electrode consisted of a platinum disk embedded in glass (2 mm diameter), the counter electrode was a platinum wire, and the reference electrode consisted of AgCl plated on Ag wire. Solutions employed during CV studies were typically 1 mM in the metal complex and 0.1 M in $[Bu_4N][PF_6]$. All potentials are reported versus the $[Cp_2Fe]^{0/+}$ couple. For all trials, $i_{p,a}/i_{p,c} = 1$ for the $[Cp_2Fe]^{0/+}$ couple, while $i_{p,c}$ increased linearly with the square root of the scan rate (i.e., $\sqrt{\nu}$). Redox couples which exhibited behavior similar to the $[Cp_2Fe]^{0/+}$ couple were thus considered reversible.

^{t}BuNHC(Ph)=CHC(Ph)O. To a yellow solution of diphenylpropynone (1.0972 g, 0.0053 mol) in toluene (20 mL) was added *tert*-butylamine (6.0 mL, 0.057 mol) and $Zn(OTf)_2$ (200 mg, 0.55 mmol). After heating to reflux for 48 h, the volatiles were removed in vacuo to provide a pale yellow solid. This material was extracted into Et_2O (20 mL) and filtered through a Celite column (0.5 cm ×2.0 cm) supported on glass wool. The volatiles were removed in vacuo to give a pale yellow solid which was washed with hexane (3 × 5 mL). 1.2833 g, 86% yield. ^1H NMR (C_6D_6, 25 °C, 500 MHz): δ 1.00 (s, 9H, Me), 5.82 (s, 1H, γ-CH), 7.07 (br s, 3H, aryl CH), 7.10 − 7.20 (m, 3H, aryl CH), 7.23 (s, 2H, aryl CH), 8.09 (s, 2H, aryl CH), 12.32 (s, 1H, NH). $^{13}C\{^1H\}$ NMR (C_6D_6, 25 °C, 125 MHz): δ 32.1 (Me), 54.0 (*C*Me), 96.0 (γ-C), 128.0, 128.7, 128.8, 129.0, 129.1, 131.1, 138.8, 141.4, 166.8 (β-CN), 188.1 (β-CO). EI^+ MS: *m*/z 279. UV−vis (CH_2Cl_2, 6.4 × 10^{-5} M): 355 nm (ε = 11600 L mol^{-1} cm^{-1}).

^{t}BuNC(Ph)CHC(Ph)OSiMe$_3$. To a Et_2O solution (3 mL) of ^{t}BuNHC(Ph)CHC(Ph)O (53 mg, 0.19 mmol) was added $NaN(SiMe_3)_2$ (35 mg, 0.19 mmol). The solution immediately turned pale pink. Me_3SiCl (50 μL, 0.39 mmol) was then added to the reaction mixture, and the solution underwent a color change to yellow. After 2 h of stirring, the solution was filtered through a Celite column (0.5 cm ×2.0 cm) supported on glass wool, and all volatiles were removed in vacuo to provide a yellow oil. The product was extracted into hexanes (3 mL) and refiltered through a Celite column (0.5 cm ×2.0 cm) supported on glass wool. The volatiles were removed in vacuo to give a yellow oil (54 mg, 81% yield). ^1H NMR (C_6D_6, 25 °C, 500 MHz): δ −0.16 (s, 9H, SiMe), 1.56 (s, 9H, Me), 6.16 (s, 1H, γ-CH), 6.92 − 7.42 (s, 6H, aryl CH), 7.56 (s, 2H, aryl CH), 8.12 (s, 2H, aryl CH). $^{13}C\{^1H\}$ NMR (C_6D_6, 25 °C, 125 MHz): δ 1.0 (SiMe), 31.3 (Me), 35.5 (*C*Me), 107.3 (γ-C), 126.6, 129.0, 129.2, 129.3, 129.5, 139.5, 142.8, 152.6 (β-CN), 160.5 (β-CO). One aryl CH resonance was not observed. EI^+ MS: *m*/z 351.

$UO_2(^{tBu}acnac)_2$ (1). To a Et_2O solution (3 mL) of ^{t}BuNHC(Ph)=CHC(Ph)O (80 mg, 0.287 mmol) was added $UO_2(N\{SiMe_3\}_2)_2(THF)_2$ (104 mg, 0.141 mmol). The solution immediately turned orange, concomitant with the deposition of orange solid. After 24 h of stirring, the supernatant was decanted off, and the orange powder was washed with Et_2O (2 × 5 mL) and dried in vacuo (78 mg, 67% yield). Analytically pure material was grown from a solution of dichloromethane and hexane. Anal. Calcd for $UO_4N_2C_{38}H_{40}\cdot 2CH_2Cl_2$: C, 48.21; H, 4.45; N, 2.81 Found: C, 49.16; H, 4.34; N, 3.05. ^1H NMR (C_6D_6, 25 °C, 500 MHz): δ 1.73 (s, 18H, Me), 5.81 (s, 2H, γ-CH), 6.99 (br s, 6H, aryl CH), 7.11 − 7.18 (br s, 4H, aryl CH), 7.20 (br s, 6H, aryl CH), 8.17 (br s, 4H, aryl CH). $^{13}C\{^1H\}$ NMR (CD_2Cl_2, 25 °C, 125 MHz): δ 33.6 (Me), 102.9 (γ-C), 127.6, 127.9, 128.4, 129.0, 130.6, 131.1, 139.7, 146.5, 171.8 (β-CN), 173.4 (β-CO). The (*C*Me) resonance was not observed. UV−vis (CH_2Cl_2, 3.1 × 10^{-5} M): 343 nm (ε = 18900 L mol^{-1} cm^{-1}). IR (KBr pellet, cm^{-1}): 1608(m), 1588(s), 1562(s), 1481(s), 1459(s), 1396(w), 1383(m), 1367(m), 1341(s), 1303(w), 1276(m), 1241(w), 1227(m), 1197(s), 1135(w), 1077(w), 1059(m), 1027(m), 1003(w), 973(w), 907(s, $\nu_{asym}(U{=}O)$), 857(w), 815(w), 758(s), 705(s), 694(s), 626(w), 594(w), 554(m), 532(m), 502(m). Raman (cm^{-1}): 823 (s, $\nu_{sym}(U{=}O)$).

[Ph$_3$PI][U(OSiMe$_3$)$_2$I$_4$] (2). To an orange suspension of **1** (135 mg, 0.163 mmol) in toluene (3 mL) was added Me_3SiI (240 μL, 1.90 mmol). The solution immediately turned deep red. After stirring for 60 min, the solution was filtered through a Celite column (0.5 cm ×2.0 cm) supported on glass wool. Triphenylphosphine (44 mg, 0.17 mmol) was then added to the reaction mixture. After 15 min of stirring the deposition of black microcrystalline material was observed. The solid was isolated and extracted into dichloromethane (3 mL). Storage of this solution at −25 °C for 24 h resulted in the deposition of black crystals suitable for X-ray analysis (85 mg, 40% yield). The reaction can also be performed in the presence of 0.5 equiv of Ph_3P; however, the isolated yield is slightly reduced (34%). Anal. Calcd for $UO_2C_{24}H_{33}Si_2P_1I_5$: C, 21.95; H, 2.53; N, 0.00. Found: C, 22.43; H, 2.20; N, <0.2. ^1H NMR (CD_2Cl_2, 25 °C, 500 MHz): δ 2.17 (s, 18H, Me), 4.03 (s, 18H, Me), 7.38 (q, 6H, J_{HH} = 7.7 Hz, ortho CH), 7.61 (br s, 6H, meta CH), 7.77 (t, 3H, J_{HH} = 7.1 Hz, para CH). $^{31}P\{^1H\}$ NMR: (CD_2Cl_2, 25 °C, 202 MHz): δ 11.6 (br s). UV−vis/NIR (CH_2Cl_2, 4.5 × 10^{-3} M): 1102 nm (ε = 10 L mol^{-1} cm^{-1}), 1478 nm (ε = 6.6 L mol^{-1} cm^{-1}), 1570 nm (ε = 11 L mol^{-1} cm^{-1}), 1664 nm (ε = 4.0 L mol^{-1} cm^{-1}). IR (KBr pellet, cm^{-1}): 1480(w), 1437(m), 1367(w), 1351(w), 1252(s), 1164(m), 1125(s), 1102(s), 1067(s), 997(m), 924(m), 851(s), 812(s), 756(s), 725(s), 689(s),

dx.doi.org/10.1021/ic200387n |*Inorg. Chem.* 2011, 50, 5105–5112

543(w), 522(w), 501(w), 465(w). Evans method (CD_2Cl_2, 0.028 M, 22 °C): μ_{eff} = 1.4 μ_B.

$U(OSiMe_3)_2I_2(bipy)_2$ (3). To a black suspension of **2** (56 mg, 0.043 mmol) in toluene (3 mL) was added bipyridine (14 mg, 0.090 mmol) in toluene (1 mL). Over 40 min, the solution undergoes a color change to orange, concomitant with the deposition of yellow solid. After 40 min, the solution was filtered through a Celite column (0.5 cm ×2.0 cm) supported on glass wool. The supernatant was concentrated in vacuo to 2 mL. Storage of this solution at −25 °C for 24 h resulted in the deposition of orange microcrystalline powder. The product was isolated by decanting off the supernatant and drying in vacuo (36 mg, 85% yield). Crystals suitable for X-ray analysis were grown from a solution of dichloromethane and hexane (1:4 v/v). Anal. Calcd for $UO_2C_{26}H_{34}N_4Si_2I_2$: C, 31.78; H, 3.49; N, 5.70. Found: C, 32.79; H, 3.78; N, 4.98. ^{1}H NMR (CD_2Cl_2, 25 °C, 500 MHz): δ −28.68 (s, 4H, aryl CH), −19.63 (s, 4H, aryl CH), −3.01 (s, 4H, aryl CH), −2.75 (s, 4H, aryl CH), 52.14 (s, 18H, Me). UV−vis/NIR (CH_2Cl_2, 4.9 × 10^{-3} M): 690 nm (ε = 18 L mol^{-1} cm^{-1}), 736 nm (ε = 19 L mol^{-1} cm^{-1}), 790 nm (ε = 21 L mol^{-1} cm^{-1}), 928 nm (ε = 17 L mol^{-1} cm^{-1}), 1004 nm (ε = 15 L mol^{-1} cm^{-1}), 1070 nm (ε = 47 L mol^{-1} cm^{-1}), 1156 nm (ε = 35 L mol^{-1} cm^{-1}), 1334 nm (ε = 48 L mol^{-1} cm^{-1}), 1388 nm (ε = 25 L mol^{-1} cm^{-1}), 1452 nm (ε = 26 L mol^{-1} cm^{-1}), 1670 nm (ε = 6.4 L mol^{-1} cm^{-1}). IR (KBr pellet, cm^{-1}): 1598(m), 1563(w), 1526(w), 1510(w), 1495(w), 1475(w), 1437(s), 1316(m), 1244(s), 1174(w), 1156(m), 1103(m), 1064(m), 1045(w), 1012(s), 928(s), 877(s), 864(s), 834(s), 763(s), 736(s), 695(m), 644(m), 627(w), 468(m), 419(m). Evans method (CD_2Cl_2, 0.010 M, 22 °C): μ_{eff} = 2.7 μ_B.

The yellow solid produced during the reaction was extracted into dichloromethane (2 mL) and layered with hexanes. Storage of this solution at −25 °C for 24 h resulted in the deposition of yellow needles (13 mg, 60% yield). These were determined to be $[Ph_3PI][I]$ by comparison with the authentic material. ^{1}H NMR (CD_2Cl_2, 25 °C, 500 MHz): δ 7.60 (br m, 12H, aryl CH), 7.71 (br s, 3H, aryl CH, J_{HH} = 6.4 Hz). $^{31}P\{^1H\}$ NMR: (CD_2Cl_2, 25 °C, 202 MHz): δ −19.6 (br s).

$U(OSiMe_3)_2I_2(phen)_2$ (4). To a black suspension of **2** (40 mg, 0.031 mmol) in toluene (3 mL) was added phenanthroline (11 mg, 0.061 mmol) in toluene (1 mL). After 10 min the solution undergoes a color change to orange concomitant with the deposition of yellow solid. The solution was filtered through a Celite column (0.5 cm ×2.0 cm) supported on glass wool. The volatiles were removed in vacuo leaving a dark red-orange oil. This material was extracted into dichloromethane (2 mL) and filtered through a Celite column (0.5 cm ×2.0 cm) supported on glass wool. The supernatant was then layered with diethyl ether (2 mL). Subsequent storage of this solution at −25 °C for 24 h resulted in the deposition of orange microcrystalline solid. The product was isolated by decanting off the supernatant and drying in vacuo (18 mg, 56% yield). Anal. Calcd for $UO_2C_{30}H_{34}N_4Si_2I_2$: C, 34.96; H, 3.33; N, 5.43. Found: C, 35.02; H, 3.35; N, 4.99. ^{1}H NMR (CD_2Cl_2, 25 °C, 500 MHz): δ −6.20 (s, 4H, aryl CH), −1.58 (s, 4H, aryl CH), 0.75 (s, 4H, aryl CH), 45.64 (s, 18H, Me). One of the aryl resonances was not observed. UV−vis/NIR (CH_2Cl_2, 3.7 × 10^{-3} M): 682 nm (ε = 32 L mol^{-1} cm^{-1}), 800 nm (ε = 27 L mol^{-1} cm^{-1}), 920 nm (ε = 31 L mol^{-1} cm^{-1}), 1006 nm (ε = 34 L mol^{-1} cm^{-1}), 1068 nm (ε = 46 L mol^{-1} cm^{-1}), 1180 nm (ε = 52 L mol^{-1} cm^{-1}), 1334 nm (ε = 56 L mol^{-1} cm^{-1}), 1376 nm (ε = 45 L mol^{-1} cm^{-1}), 1666 nm (ε = 17 L mol^{-1} cm^{-1}). IR (KBr pellet, cm^{-1}): 1590(w), 1517(w), 1543(w), 1519(m), 1498(w), 1476(w), 1473(w), 1460(w), 1453(w), 1423(m), 1348(w), 1246(m), 1223(w), 1143(m), 1103(m), 997(w), 930(s), 865(s), 846(s), 777(w), 752(m), 727(s), 690(w), 637(w), 543(w), 579(w), 500(m), 418(m).

The yellow solid produced during the reaction was extracted into dichloromethane (2 mL) and layered with hexane (2 mL). Storage of this solution at −25 °C for 24 h resulted in the deposition of dull yellow powder determined to be $[Ph_3PI][I]$ by comparison with the authentic material (10 mg, 63% yield).

$[U(OSiMe_3)_2I(THF)_4][I_3]$ (5). Complex **2** (36 mg, 0.027 mmol) was dissolved in THF (2 mL), immediately forming an orange solution. After 5 min the solution was filtered through a Celite column (0.5 cm ×2.0 cm) supported on glass wool and layered with hexane (4 mL). Storage of this solution at −25 °C for 24 h resulted in the cocrystallization of yellow needles and orange needles. The total mass of material collected was 25.8 mg. The yellow needles were determined to be $[Ph_3PI][I]$ by comparison with the spectral properties of the independently prepared material.[17] The orange needles were determined to be $[U(OSiMe_3)_2I(THF)_4][I_3]$ (**5**) by X-ray crystallography. Because of similar solubility properties of $[Ph_3PI][I]$ and complex **5**, isolation of pure samples of **5** proved unsuccessful. As such, characterization was performed on the mixture of $[Ph_3PI][I]$ and complex **5**. ^{1}H NMR (CD_2Cl_2, 25 °C, 500 MHz): δ 7.40 (br m, 6H, aryl CH), 7.59 (br m, 6H, aryl CH), 7.74 (br m, 3H, aryl CH), 58.10 (s, 18H, Me). $^{31}P\{^1H\}$ NMR (CD_2Cl_2, 25 °C, 202 MHz): δ −1.11 (br s). $^{31}P\{^1H\}$ NMR (THF-h_8, 25 °C, 202 MHz): δ −20.8 (br s). IR (KBr pellet, cm^{-1}): 1591(w), 1562(w), 1544(w), 1528(w), 1510(w), 1500(w), 1477(w), 1460(w), 1437(m), 1336(w), 1313(w), 1253(m), 1183(w), 1165(w), 1122(s), 1101(m), 1053(s), 1039(s), 1015(s), 996(s), 926(w), 877(s), 844(s), 748(m), 727(s), 688(s), 618(w), 608(w), 540(s), 518(w), 499(s), 445(w), 421(w).

X-ray Crystallography. Data for **1**·$2CH_2Cl_2$, **2**, **3**·CH_2Cl_2, and **5** were collected on a Bruker 3-axis platform diffractometer equipped with a SMART-1000 CCD detector using a graphite monochromator with a Mo Kα X-ray source (α = 0.71073 Å). The crystals were mounted on a glass fiber under Paratone-N oil, and all data were collected at 150(2) K using an Oxford nitrogen gas cryostream system. A hemisphere of data was collected using ω scans with 0.3° frame widths. Frame exposures of 25, 10, 10, and 35 s were used for complexes **1**·$2CH_2Cl_2$, **2**, **3**·CH_2Cl_2, and **5**, respectively. Data collection and cell parameter determination was conducted using the SMART program.[41] Integration of the data frames and final cell parameter refinement was performed using the SAINT software.[42] Absorption correction of the data was carried out empirically based on reflection ψ-scans. Subsequent calculations were carried out using SHELXTL.[43] Structure determination was done using direct methods and difference Fourier techniques. All hydrogen atom positions were idealized, and rode on the atom of attachment. Structure solution, refinement, graphics, and creation of publication materials were performed using SHELXTL.[43] Complex **3** contains a disordered molecule of CH_2Cl_2, which was modeled over two positions in a 50:50 ratio. In addition, complex **5** contains two disordered THF ligands, each of which were modeled over two positions, in a 50:50 ratio. Finally, one silyloxide ligand in **5** was found to be disordered between two positions about the silicon atom, also in a 50:50 ratio. Idealized hydrogen atoms were not assigned to the disordered carbon atoms. A summary of relevant crystallographic data for **1**·$2CH_2Cl_2$, **2**, **3**·CH_2Cl_2, and **5** is presented in Table 1.

■ ASSOCIATED CONTENT

Supporting Information. Crystallographic details (as CIF files) for **1**·$2CH_2Cl_2$, **2**, **3**·CH_2Cl_2, and **5**, tabulated cyclic voltammetry data for **1**·$2CH_2Cl_2$, and spectral data **1**·$2CH_2Cl_2$, **2**, **3**·CH_2Cl_2, **4**, and **5**. This material is available free of charge via the Internet at http://pubs.acs.org.

■ AUTHOR INFORMATION

Corresponding Author

*E-mail: hayton@chem.ucsb.edu.

■ ACKNOWLEDGMENT

We thank the University of California, Santa Barbara, and the Department of Energy (BES Heavy Element Program) for financial support of this work.

■ REFERENCES

(1) Arnold, P. L.; Patel, D.; Wilson, C.; Love, J. B. *Nature* **2008**, *451*, 315–318.
(2) Brown, J. L.; Wu, G.; Hayton, T. W. *J. Am. Chem. Soc.* **2010**, *132*, 7248–7249.
(3) Berthet, J. C.; Siffredi, G.; Thuery, P.; Ephritikhine, M. *Eur. J. Inorg. Chem.* **2007**, 4017–4020.
(4) Arnold, P. L.; Love, J. B.; Patel, D. *Coord. Chem. Rev.* **2009**, *253*, 1973–1978.
(5) Yahia, A.; Arnold, P. L.; Love, J. B.; Maron, L. *Chem. Commun.* **2009**, 2402–2404.
(6) Yahia, A.; Arnold, P. L.; Love, J. B.; Maron, L. *Chem.—Eur. J.* **2010**, *16*, 4881–4888.
(7) Walsh, R. *Acc. Chem. Res.* **1981**, *14*, 246–252.
(8) Hayton, T. W.; Wu, G. *Inorg. Chem.* **2009**, *48*, 3065–3072.
(9) Schnaars, D. D.; Wu, G.; Hayton, T. W. *J. Am. Chem. Soc.* **2009**, *131*, 17532–17533.
(10) Santhosh Kumar, K. S.; Li, Y.; Gnanou, Y.; Baish, U.; Champouret, Y.; Poli, R.; Robson, K. C. D.; McNeil, W. S. *Chem. Asian J.* **2009**, *4*, 1257–1265.
(11) Holm, R. H.; Parks, J. E. *Inorg. Chem.* **1968**, *7*, 1408–1416.
(12) Stabnikov, P. A.; Zharkova, G. I.; Baidina, I. A.; Tkachev, S. V.; Krisyuk, V. V.; Igumenov, I. K. *Polyhedron* **2007**, *26*, 4445–4450.
(13) Lee, D. H.; Hwang, Y. J.; Yoon, J. S.; Choi, M. K.; Lee, I.-M. *Bull. Korean Chem. Soc.* **2009**, *30*, 636–646.
(14) Fouli, F. A.; Beshay, A. D. *Indian J. Chem.* **1980**, *19B*, 410–412.
(15) Nocton, G.; Horeglad, P.; Vetere, V.; Pecaut, J.; Dubois, L.; Maldivi, P.; Edelstein, N. M.; Mazzanti, M. *J. Am. Chem. Soc.* **2010**, *132*, 495–508.
(16) Takao, K.; Kato, M.; Takao, S.; Nagasawa, A.; Bernhard, G.; Hennig, C.; Ikeda, Y. *Inorg. Chem.* **2010**, *49*, 2349–2359.
(17) Bricklebank, N.; Godfrey, S. M.; Mackie, A. G.; McAuliffe, C. A.; Pritchard, R. G.; Kobryn, P. J. *J. Chem. Soc., Dalton Trans.* **1993**, 101–103.
(18) Godfrey, S. M.; Kelly, D. G.; McAuliffe, C. A.; Mackie, A. G.; Pritchard, R. G.; Watson, S. M. *J. Chem. Soc., Chem. Commun.* **1991**, 1163–1164.
(19) Bricklebank, N.; Godfrey, S. M.; McAuliffe, C. A.; Pritchard, R. G. *J. Chem. Soc., Dalton Trans.* **1993**, 2261–2266.
(20) Pritchard, R. G.; Moreland, L. *Acta Crystallogr.* **2006**, *C62*, 0656–0658.
(21) Cotton, F. A.; Kibala, P. A. *J. Am. Chem. Soc.* **1987**, *109*, 3308–3312.
(22) Evans, D. F. *J. Chem. Soc.* **1959**, 2003–2005.
(23) Catro-Rodriguez, I.; Meyer, K. *Chem. Commun.* **2006**, 1353–1368.
(24) Duval, P. B.; Burns, C. J.; Clark, D. L.; Morris, D. E.; Scott, B. L.; Thompson, J. D.; Werkema, E. L.; Jia, L.; Anderson, R. A. *Angew. Chem., Int. Ed.* **2001**, *40*, 3462–3465.
(25) Graves, C. R.; Vaughn, A. E.; Schelter, E. J.; Scott, B. L.; Thompson, J. D.; Morris, D. E.; Kiplinger, J. L. *Inorg. Chem.* **2008**, *47*, 11879–11891.
(26) Ryan, J. L. *J. Inorg. Nucl. Chem.* **1971**, *33*, 153–177.
(27) Muetterties, E. L.; Guggenberger, L. J. *J. Am. Chem. Soc.* **1974**, *96*, 1748–1756.
(28) Berthet, J. C.; Nierlich, M.; Ephritikhine, M. *Dalton Trans.* **2004**, 2814–2821.
(29) Schettini, M. F.; Wu, G.; Hayton, T. W. *Inorg. Chem.* **2009**, *48*, 11799–11808.
(30) Shinomoto, R.; Zalkin, A.; Edelstein, N. M.; Zhang, D. *Inorg. Chem.* **1987**, *26*, 2868–2872.
(31) Karmazin, L.; Mazzanti, M.; Bezombes, J.-P.; Gateau, C.; Pecaut, J. *Inorg. Chem.* **2004**, *43*, 5147–5158.
(32) Monreal, M. J.; Diaconescu, P. L. *Organometallics* **2008**, *27*, 1702–1706.
(33) Cohen, D.; Carnall, W. T. *J. Phys. Chem.* **1960**, *64*, 1933–1936.
(34) Morss, L. R.; Edelstein, N. M.; Fuger, J.; Katz, J. J. *The Chemistry of the Actinide and Transactinide Elements*; Springer: Dordrecht, The Netherlands, 2006.
(35) Fortier, S.; Melot, B. C.; Wu, G.; Hayton, T. W. *J. Am. Chem. Soc.* **2009**, *131*, 15512–15521.
(36) Nocton, G.; Pecaut, J.; Filinchuk, Y.; Mazzanti, M. *Chem. Commun.* **2010**, *46*, 2757–2759.
(37) Bent, H. A. *Chem. Rev.* **1968**, *68*, 587–648.
(38) Avens, L. R.; Barnhart, D. M.; Burns, C. J.; McKee, S. D. *Inorg. Chem.* **1996**, *35*, 537–539.
(39) Fortier, S.; Hayton, T. W. *Coord. Chem. Rev.* **2010**, *254*, 197–214.
(40) Andersen, R. A. *Inorg. Chem.* **1979**, *18*, 209–209.
(41) *SMART Software Users Guide*, Version 5.1; Bruker Analytical X-ray Systems Inc.: Madison, WI, 1999.
(42) *SAINT Software Users Guide*, Version 5.1; Bruker Analytical X-ray Systems Inc.: Madison, WI, 1999.
(43) Sheldrick, G. M. *SHELXTL*, 6.12; Bruker Analytical X-ray Systems Inc.: Madison, WI, 2001.